Journal of
MATERIALS RESEARCH

Influence of deposition parameters on mechanical properties of sputter-deposited Cr_2O_3 thin films

P. Hones and F. Lévy
EPFL-Institut de physique appliquée, Ecole Polytechnique Fédérale de Lausanne, CH-1015 Lausanne, Switzerland

N.X. Randall
CSEM Instruments, Jaquet-Droz 1, CH-2007 Neuchâtel, Switzerland

Among the oxides, Cr_2O_3 exhibits the highest hardness value and a low coefficient of friction. These properties make chromium oxide an excellent coating material for tribological applications. Cr_2O_3 thin films were deposited by radio-frequency reactive magnetron sputtering at substrate temperature in the range 363–593 K. The hardness and elastic modulus of the films were measured by two complementary nanoindentation techniques to investigate the influences of the substrate temperature and the oxygen content in the sputtering gas. While the continuous stiffness data method provides information throughout the whole film thickness, nanoindentation combined with scanning force microscopy of the residual imprints allows visualization of pileup, cracking, and delamination from the substrate. Hardness values up to 32 GPa were obtained for substrate temperatures exceeding 500 K and oxygen contents between 15% and 25% of the total gas pressure. The films, obtained with these deposition conditions, showed good adhesion to silicon substrates.

I. INTRODUCTION

It has been established that Cr_2O_3 is among the hardest oxides both in the mineralogical (8.5 Mohs) and in the microhardness scales (29.5 GPa).[1] However, recent research work has concentrated mostly on Al_2O_3, which is used in tribological and microelectronic applications as a barrier layer, due to its chemical and thermodynamical stability. Comparatively few publications are dedicated to chromium oxide and its mechanical properties. Cr_2O_3 films have been deposited by sputtering, chemical vapor deposition (CVD) and plasma spray pyrolysis. Studies report a good wear resistance and a low coefficient of friction,[2] however hardness values well below the bulk value. Recently, Bhushan *et al.*[3] measured a hardness value of 29.5 GPa for a 200-nm-thick oxygen deficient film. The major drawback compared to the generally softer transition metal nitrides, which are nowadays standard in the industry of wear protective coatings, is the usually lower toughness and transverse rupture strength of the oxide coatings.[4] Nevertheless, Cr_2O_3 coatings have already found several applications e.g. as protective coatings on read-write heads in digital magnetic recording units[5] or in gas-bearing applications.[3]

The present study investigates the influence of deposition parameters, namely the substrate temperature and the oxygen content in the sputtering gas, on the mechanical properties of Cr_2O_3 thin films. In order to obtain not only accurate hardness and modulus values, but also information on the deformation mechanism, two complementary nanoindentation techniques have been used, namely the continuous stiffness method (which measures hardness as a function of depth through the coating) and conventional nanoindentation combined with scanning force microscopy (SFM). In addition, indentation experiments with constant load at different indentation depths have been performed to investigate the room temperature creeping behavior of the films.

Nanoindentation has become widely accepted in mechanical characterization of thin films as the logical refinement of microindentation. The latter is limited by the resolution of the optical microscope, which is used to determine the imprint diagonal for calculating the hardness of the tested material. The nanoindentation principle relies on the continuous measurement of force and displacement as an indenter, of known geometry, is pressed into a sample material.[6–10] The force is usually applied via an electromagnet, in which case the current in the coil determines the load, or by a piezoelectric load cell where the inherent inaccuracies in such a system are corrected by interferometry. The displacement is measured, in most cases, by a capacitive sensor. With instruments having micronewton force and nanometer depth resolutions it is possible to produce load-displacement curves representative of the material response in terms of hardness and elastic modulus.[11] However, a true understanding of the elastic/plastic interactions occurring at the indenter/sample interface is not possible solely from such data.

Additional surface topographical information has become increasingly important for characterizing surface deformation in and around the indentation area. Various

methods have been proposed, including scanning electron microscopy (SEM),[10] transmission electron microscopy (TEM),[12] and scanning tunneling microscopy (STM)/SFM.[13] The later scanning probe techniques allow measuring quantitatively interfacial effects, such as material pile-up around the indentation imprints, with nanometric precision and three-dimensional imaging capability. Furthermore, SFM does normally not require a special sample preparation or a vacuum environment, and in a stand-alone configuration it can measure samples of unlimited size.[14] Previous investigations[15] have shown the net advantages of combining nanoindentation with SFM and the present work aims introducing such a method for the characterization of Cr_2O_3 thin films.

II. EXPERIMENTAL

Cr_2O_3 thin films were prepared by reactive radio-frequency (rf) sputtering. The power density on the metallic chromium (purity 99.5%) target was 66.3 kW/m^2. The depositions were performed at a total pressure of 10^{-1} Pa in a mixed Ar and O_2 atmosphere. The ratio between the partial pressure of the reactive gas (O_2) and the total gas pressure was varied from 5% to 30% in order to obtain different oxygen concentrations in the films. Silicon wafers were used as substrates. The film thicknesses were approximately 1.8 μm. The density of the films was calculated from the thickness, the surface area, and the weight, which was determined by weighting the substrates before and after the deposition. The oxygen concentration of films was measured by electron probe microanalysis (EPMA) using the Cr K_α and the O K_α lines.[16] RuO_2 and CrN films served as standards. The crystal structure and phase were investigated by x-ray diffraction (XRD) at grazing incidence ($\theta = 4°$). The $\sin^2\Psi$ method was applied to determine the residual stress.

The nanohardness was determined with two different commercial nanoindentation systems. The Nano Instruments XP system was used to indent the films with a Berkovich-type pyramidal diamond tip to a maximum depth of 700 nm. The indentation cycle commences after a lengthy equalization period in order to minimize the influence of thermal drift. Constant stiffness data measurements are obtained by oscillating the tip during indentation at a frequency of about 62 Hz. This kind of measurement provides hardness, elastic modulus and stiffness data at regular intervals throughout the total indentation depth.[17] Overall hardness values were taken at depths in the range 200–300 nm (i.e., <15% of the film thickness) to avoid influences of the surface roughness and substrate. The reported hardness values measured with the XP instrument represent an average of 9 indentations. The indentation sites were 30 μm apart. In additional experiments, the films were indented to depths of 200, 400, or 700 nm. When the respective depth was attained the indenter displacement, which is a measure for the plastic depth in absence of any thermal drift, was recorded for 15 s at constant load. The analysis of the time dependence of the displacement provides information on creep.[18] Following earlier investigations,[19] the strain rate is defined as $\dot{\epsilon} = (1/h)(dh/dt)$ where h is the plastic indentation depth. The strain rate depends on the stress relaxation mechanism (e.g., dislocation slips, crack propagation, phase transformation) and on the material in which the relaxation takes place. In order to avoid an influence of the thermal drift, the measurements were taken in this relatively short time period after the stop of the load increase where the strain rate is time dependent, before it reaches an approximately constant value. As the measurements were performed at ambient temperature, far below the melting point of the material, this constant value is very small in ceramics. Consequently, an accurate determination of the strain rate constant is difficult and implies long measuring times, which critically require the absence of any thermal drift.

The CSEM Instruments nanoindentation apparatus consists of a Nano Hardness Tester (NHT)[20] with an integrated optical/scanning force microscope system. The NHT includes two distinct components, a measuring head for performing indentations and an optical microscope for selecting a specific sample site prior to indentation and for checking the location of the imprint after indentation. Both components are directly linked by an electro-mechanical positioning system which allows displacements along in two perpendicular horizontal axes with a resolution of 1 μm. The main advantage of this instrument is its differential measurement of the indentation depth, made possible by a sapphire reference ring which remains in contact with the sample surface during the loading/unloading cycle, giving exact positioning of the indenter tip relative to the sample surface. Thus the elasticity of the sample and holder is compensated, as well as the thermal drift during the measurement.

The SFM head is integrated within the optical microscope. The optical microscope allows the selection of a definite sample area and then to relocate it precisely under the SFM head in order to carry out high-resolution microscopy of the same area. The actual SFM used was a SIS *ULTRAobjective*™,[21] an instrument having subnanometer lateral and vertical displacement resolution.

III. RESULTS

Deposition rate is important regarding industrial applications, but depends strongly on the geometrical factors in the deposition chamber. The low deposition rates are due to the large distance between target and substrate, which presents the advantage of providing a very homogeneous deposition. The deposition rate increases slightly with the substrate temperature, T_S to a shallow maximum at about 530 K (Fig. 1). This is attributed on

https://doi.org/10.1557/JMR.1999.0489

the one hand to an increased reactivity at higher T_S and on the other hand to a decrease of the sticking coefficient of oxygen on the surface. It shows also a significant dependence on the oxygen content in the plasma. The highest deposition rate was obtained with an oxygen content of about 15% of the working gas pressure. Increasing the oxygen partial pressure further an increased target poisoning slows the deposition process down.

The density of the films is strongly dependent on the process parameters. At 363 K the films show a rather low density of 4.65 g/cm^3 compared to the Cr_2O_3 bulk value[22] of 5.21 g/cm^3 (Fig. 2). The density increases at higher substrate temperatures; at 593 K the density reaches almost the bulk value. Very large deviations from this value are observed for the films deposited at very low and very high oxygen contents in the working gas, while at intermediate oxygen partial pressures the density is constant and close to the Cr_2O_3 bulk density. The value of 7.3 g/cm^3 for the film deposited at 5% is near to the bulk value of metallic chromium (7.14 g/cm^3). The XRD pattern of this film exhibits peaks of the bcc structure only. The chemical composition measurements revealed only 9% at. oxygen in the film. Therefore, this film can be assigned to metallic chromium with incorporation of some oxygen in the lattice. At medium oxygen contents the densities are very close to the bulk density of Cr_2O_3, while the 2.8 g/cm^3 of the film deposited at 30% oxygen indicates a high porosity.

The chemical composition measurements (Fig. 3) revealed that the films deposited with an oxygen content between 10% and 30% of the total gas pressure have a stoichiometry close to Cr_2O_3. XRD revealed some indications for higher oxides in the film deposited at 30% oxygen content in the sputtering gas. This phase mixture accounts for the elevated oxygen content in this film. At intermediate oxygen contents in the sputtering gas, the α–Cr_2O_3 phase was the only phase detected by XRD. Within the experimental error of 0.15 for the stoichiometric ration, which is mainly due to the uncertainty of the chemical composition of the standards used in EPMA, these films consist of stoichiometric Cr_2O_3. The substrate temperature also has an influence on the chemical composition. At low substrate temperatures the films are only slightly overstoichiometric. These films are mainly amorphous, but contain some nanocrystalline

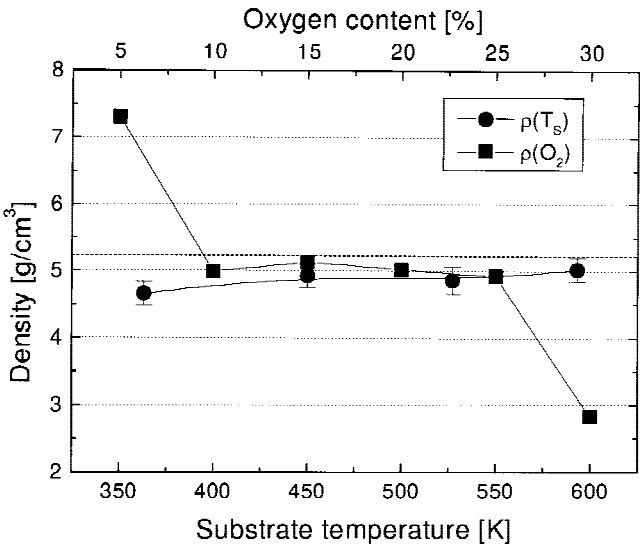

FIG. 2. CrO_x thin films: density versus oxygen content in the sputtering gas (T_S = 590 K) and the substrate temperature (at 20% oxygen content in the sputtering gas).

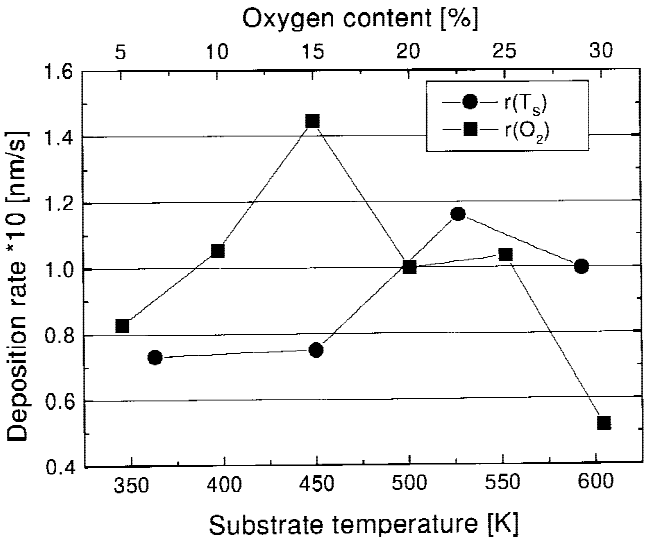

FIG. 1. CrO_x thin films: deposition rate versus oxygen content in the sputtering gas (T_S = 590 K) and the substrate temperature (at 20% oxygen content in the sputtering gas).

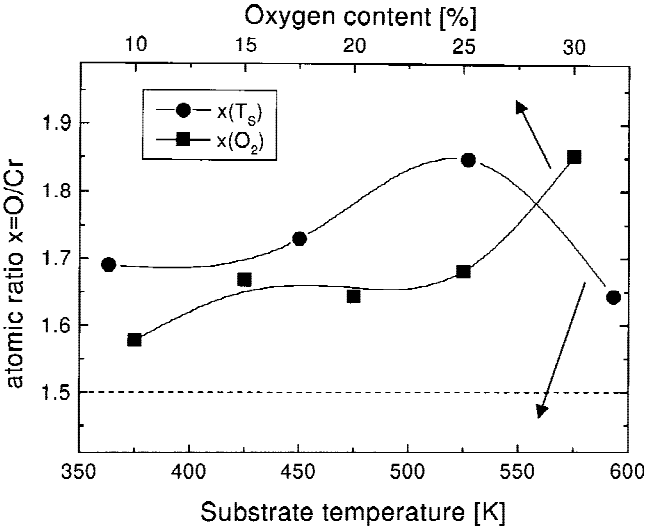

FIG. 3. CrO_x thin films: stoichiometric ratio O/Cr versus oxygen content in the sputtering gas (T_S = 590 K) and the substrate temperature (at 20% oxygen content in the sputtering gas). The solid lines are guidelines for the eye.

grains (crystallite size <7 nm). At 530 K the film is fully crystallized, but is overstoichiometric. At 590 K, a stoichiometric crystalline film is finally obtained. In every crystalline Cr_2O_3 film a compressive residual stresses below 1 GPa was measured.

In Fig. 4 the elastic modulus and hardness values are reported as a function of the substrate temperature. The amorphous films deposited at low substrate temperature exhibit a hardness value of about 20 GPa, which is close to the value reported by Kao *et al.* for the films deposited at 423 K.[23] At a substrate temperature of about 500 K, a steep increase in hardness is observed. The maximum hardness values obtained using the Nanoindenter XP and the NHT are 32 and 37 GPa, respectively. The elastic modulus of these films shows a similar dependence on the substrate temperature and exhibits the maximum values of 325 GPa with the Nanoindenter XP and 270 GPa with the NHT.

The hardness and elastic modulus reach the respective maximum values of 31 GPa (hardness) and 325 GPa (modulus) for oxygen partial pressures in the range of 15–25% of the total gas pressure (Fig. 5). At higher oxygen concentrations, both the hardness and elastic modulus decrease to the values of 2.5 and 100 GPa, respectively.

The room temperature creep experiments revealed generally a time dependence of the indenter displacement, which at constant load corresponds to the strain ϵ, given by $\epsilon = a \cdot t^{1/3}$ where a is a material and penetration depth dependent prefactor. Therefore, the strain rate $\dot{\epsilon} = (1/h)(dh/dt)$ can essentially be reduced to a strain rate prefactor $b = a/h$ in this case. This allows a simplified comparative discussion of the differences in room temperature creeping behavior of the films, as b is time-independent. Differences in the strain rate, and consequently in b, represent differences in the deformation mechanisms (e.g., crack propagation, delamination). Yurkov observed remarkable differences in the strain rate (rate of intrusion) in similar experiments on sintered Si_3N_4 and AlN ceramics,[24] which were attributed to differences in microstructure and different deformation mechanisms. With respect to thin films differences in b can also indicate a change of the medium (film or substrate) in which the deformation predominately takes place. The time dependence of the strain rate changes significantly with the indentation depth in the soft films at maximum oxygen partial pressure while it does not change in the harder films deposited at lower oxygen partial pressures (Fig. 6). The absolute values and the time dependence of the strain rate in the harder films are very similar to those of the Si substrate. The calculated strain rate prefactors of these soft films are about 4 times

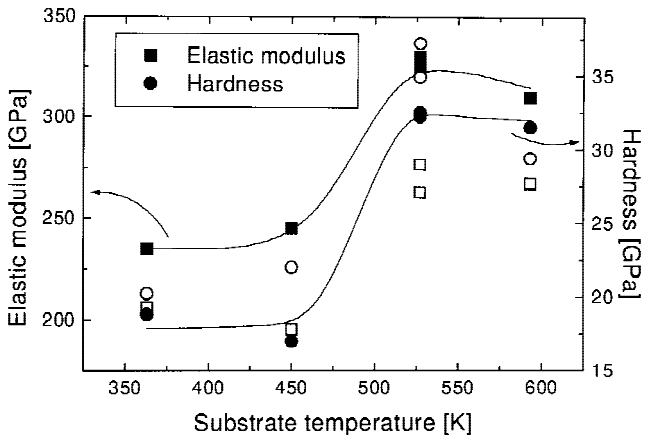

FIG. 4. Cr_2O_3 thin films: elastic modulus and hardness versus substrate temperature. The films were deposited with 20% oxygen in the sputtering gas on Si substrates. Solid symbols correspond to measurements using the Nanoindenter XP, open symbols to values obtained with the NHT. The solid lines are guidelines for the eye.

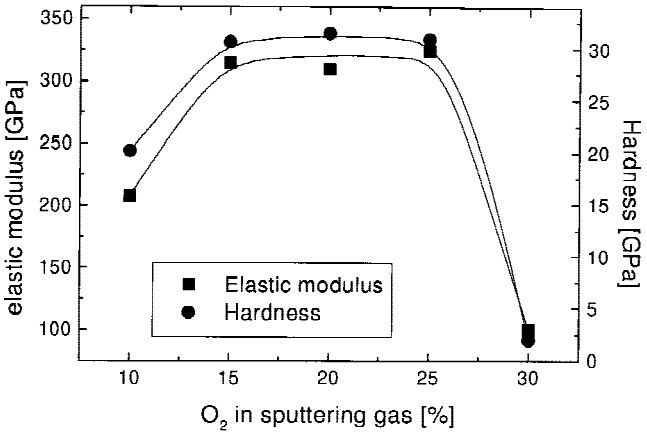

FIG. 5. Cr_2O_3 thin films: elastic modulus and hardness versus oxygen concentration in the sputtering gas. The substrate temperature was kept constant at 590 K during the deposition.

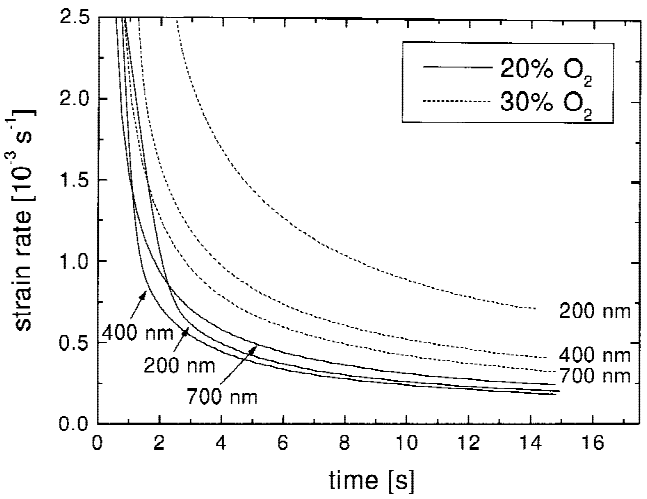

FIG. 6. Time dependence of the strain rate at constant load at different indentation depths. A hard film deposited with an oxygen partial pressure of 20% of the total working gas pressure is compared with a soft film deposited with an oxygen partial pressure of 30%. The substrate temperature during the deposition was in both cases 590 K.

higher at 200 nm, 2 times higher at 400 nm and 25% higher at 700 nm compared to those of the harder films or the Si substrate. With regard to the substrate temperature (Fig. 7), *b* is reduced to about the value of the Si substrate with increasing T_S, but does not vary significantly with the indentation depth.

Combined nanoindentation/SFM data provide additional information about the critical loads at which cracking and delamination occur. Indentation results (Fig. 8) of the Cr_2O_3 thin film deposited at $T_S = 360$ K and 20% O_2 partial pressure illustrate that above a critical load of approximately 80 mN the film begins to crack and then completely spalls off the substrate as the load is further increased. This phenomenon is identified by a flat on the loading curve, which corresponds to a stress relaxation and an absorption of energy through the local disintegration process of the film.[25] At higher loads the measured mechanical properties can therefore be mainly attributed to the Si substrate material. The Cr_2O_3 thin film deposited at $T_S = 450$ K and with 20% O_2 partial pressure, represented in Fig. 9, tends to crack laterally away from the indentation site [Fig. 9(a)] and decoheres from the substrate due to the stress at the film/substrate interface. This type of failure is sometimes attributed as pileup, but is clearly due to delamination [Fig. 9(b)] of the coating from the substrate. However, it is important to notice that films deposited at temperatures exceeding 500 K do not exhibit such brittle properties.

IV. DISCUSSION

The mechanical properties of the Cr_2O_3 films strongly depend on the deposition parameters. In particular the hardness and elastic modulus steeply drop for oxygen partial pressures exceeding 25% of the total gas pressure. SFM analysis confirms the soft nature of such coatings and their randomly oriented polycrystalline structure. For low penetration depths (i.e., less than 10% of the coating thickness), very low hardness and elastic modulus values of 2.6 and 111 GPa, respectively, were measured and coincide with a low density value (~2.8 g/cm^3) and an increased strain rate prefactor *b*. This low density value is attributed to high porosity and voids, which result in a lack of coherence of the grains and, consequently, in a low hardness value[4] and a strong room temperature creeping, At higher penetration depths, the hardness, the elastic modulus and the strain rate prefactor tend toward the values of the Si substrate indicating the strong influence of the substrate on these values. Much higher density values (4.8–5.0 g/cm^3) are obtained for films with lower oxygen concentrations. The dense films, especially those deposited at high T_S, exhibit high hardness (21–37 GPa) and elastic modulus (200–268 GPa) values and a strain rate prefactor close to that of Si. This suggests that the stress relaxation takes place mainly in the comparably softer substrate [H(Si) = 13 GPa] even at very low indentation depths. Films deposited at comparatively low substrate temperatures are more susceptible to cracking at the coating/substrate interface. This is presumably because of stress mismatches and low adhesion, which are a result of only limited interdiffusion in the interfacial zone at these temperatures. The creep experiments confirm this assumption, as these films show a higher *b* almost independently of the indentation depth, which leads to the conclusion that the stress relaxation behavior of the substrate merely influences *b* in this case. This is only possible if the coupling between film and substrate is weak, which is the case in partly delaminated films or if the predominate stress relaxation mechanism is the delamination. Furthermore, SFM images of residual imprints of indentations confirm that interfacial cracking is most prominent in the case of very low substrate temperatures (360 K) where the surrounding material completely delaminates from the Si substrate [see Fig. 8(b)]. By comparing the SFM images of residual indentations made with a maximum applied load of 200 mN, a correlation can be established between the substrate temperature and the extent of delamination around the indentation site: the higher the substrate temperature, the lower the effects of subsurface cracking. An explanation for this phenomenon is that the interdiffusion at the film/substrate interface is increased at higher deposition temperatures and strengthens the adhesion to the substrate.[4]

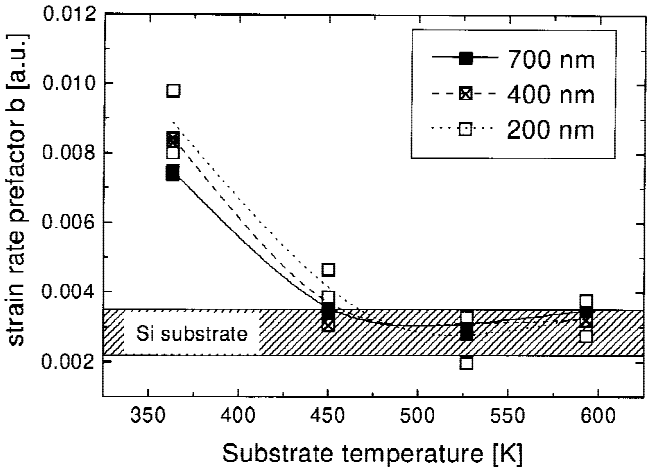

FIG. 7. Strain rate prefactor versus substrate temperature during the deposition at different indentation depths. The ≈1.8-μm-thick films were deposited with an oxygen partial pressure of 20% of the total sputtering gas pressure. The range of strain rate prefactors of the Si substrate at the different indentation depths were added for comparison.

The differences in the absolute values of the hardness and the elastic modulus between the results from the XP and the NHT apparatus (Fig. 4) origin from the differences in the analysis of the raw data. Thereby, the continuous stiffness method has the advantage that it is

https://doi.org/10.1557/JMR.1999.0489

easier to control the accuracy of the result (usually 10% for the elastic modulus and 5% for the hardness) as it provides data throughout the whole indentation depth. The hardness or elastic modulus values at only little different indentation depths of the same indentation site can be averaged and compared. In addition, the reported values in Fig. 4 represent an average over a different number of indentations (9 in the case of the Nanoindenter XP, 3

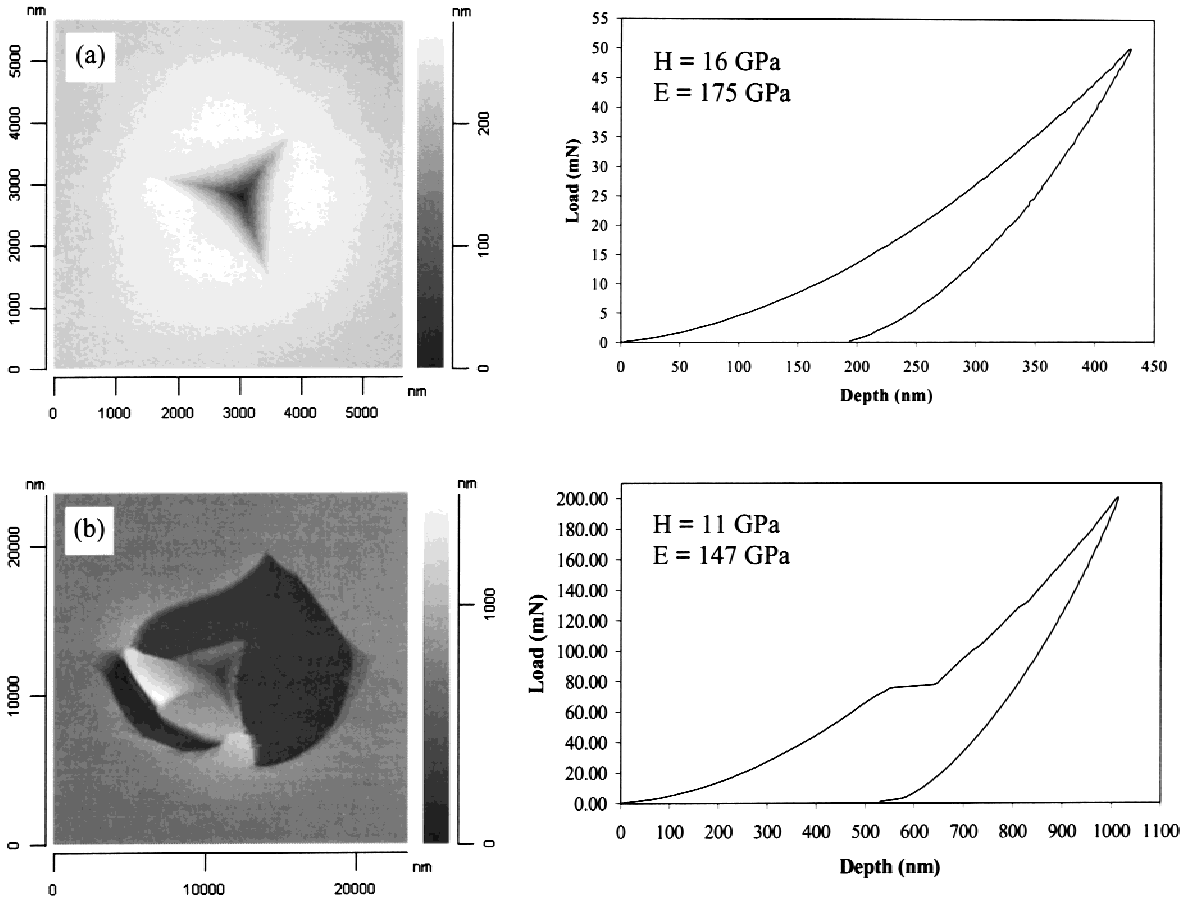

FIG. 8. Berkovich indentation data for a Cr_2O_3 thin film deposited at a substrate temperature of 360 K and with a 20% O_2 sputtering gas concentration. Example (a) shows a 50-mN monocycle, whereas (b) shows the cracking and delamination effects that occur above a critical applied load of approximately 80 mN. At higher loads the measured mechanical properties are almost entirely those of the Si substrate.

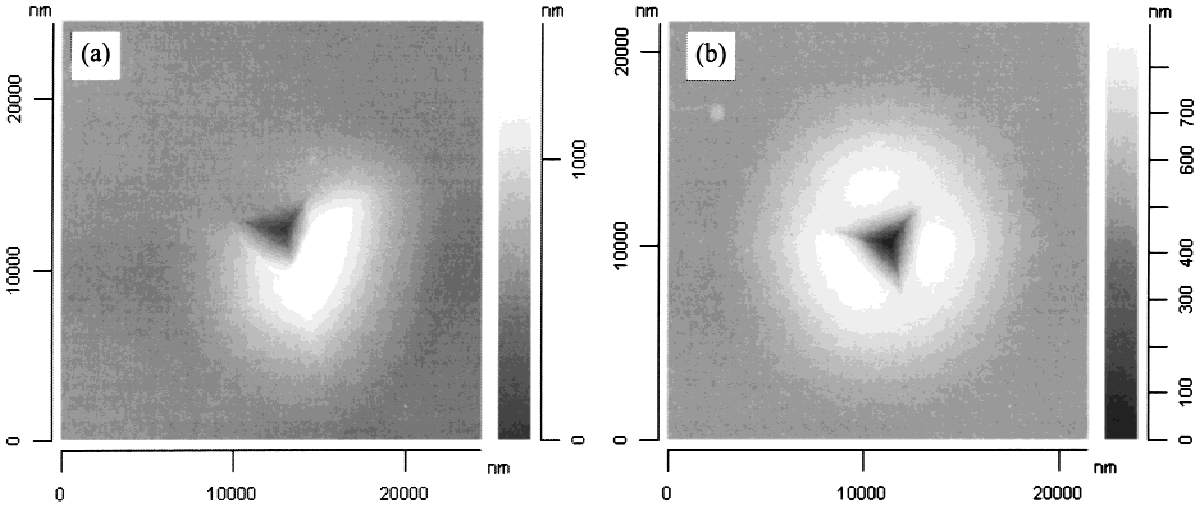

FIG. 9. SFM images for indentations made at maximum loads of 200 mN for a Cr_2O_3 thin film deposited at a substrate temperature of 450 K and with a 20% O_2 sputtering gas concentration. Note the lateral cracking (a) and pile-up/delamination (b) around the indentation site at such high loads.

in the case of the NHT). This illustrates that a quantitative comparison of hardness and modulus values measured with a different apparatus and analysis has to be handled with caution.

V. CONCLUSIONS

Regarding the investigation techniques, it is very difficult to determine the true deformation mechanisms occurring at the tip-sample interface unambiguously with load-displacement measurements alone. SFM imaging of the residual imprints at various depths is a viable and successful approach to characterize the coating-substrate deformation behavior. In addition, the NHT/SFM combination is capable of providing load-displacement data together with topographical information (i.e., surface roughness, extent of pileup/sink-in effects, cracking, true area of contact, volume of material displaced, etc.) in a fast and efficient manner. Additional information on the deformation mechanism can also be deduced from a room temperature creep analysis at constant load.

Regarding the Cr_2O_3 coatings, a clear correlation has been established between the mechanical properties of the tested Cr_2O_3 thin films and the deposition parameters. The present study reveals optimum deposition conditions with an oxygen content of about 15% in the sputtering gas at substrate temperatures exceeding 500 K. Under these conditions stoichiometric Cr_2O_3 films are deposited at the highest deposition rates. They exhibit hardness values exceeding 30 GPa while still adhering well to the substrate.

ACKNOWLEDGMENTS

This work was supported by the Fonds National Suisse de la Recherche Scientifique and the Board of the Swiss Federal Institute of Technology (Priority program in Materials Research). Particular thanks are due to C. Zakri and A. Gentile for experimental support and Dr. François Bussy at the Université de Lausanne for the electron probe microanalysis measurements. M. Diserens, J. Michler and A. Karimi are greatly acknowledged for helpful discussions.

REFERENCES

1. G.V. Samsonov, *The Oxide Handbook*, 2nd ed. (IFI/Plenum, New York, 1982), pp. 192, 195.
2. J.L. Zhang, J. Huang and C. Ding, J. Therm. Spray Technol. **7,** 242 (1998).
3. B. Bhushan, G.S. Theunissen, and X. Li, Thin Solid Films **311,** 67 (1997).
4. J-E. Sundgren and H.T.G. Hentzell, J. Vac. Sci. Technol, A **4,** 2259 (1986).
5. V. Zieren, M.d. Jongh, A.B.v. Groenou, J.B.v. Zon, P. Lansinski, and G.S. Theunissen, IEEE Trans. Magn. **30,** 340 (1994).
6. J. Loubet, J.M. Georges, D. Marchesini, and G. Meille, J. Tribology **106,** 43 (1984).
7. T.F. Page, W.C. Oliver, and C.J. McHargue, J. Mater. Res. **7,** 450 (1992).
8. B. Bhushan, V.S. Williams, and R.V. Shack, Trans. ASME J. Tribol. **110,** 563 (1988).
9. M. Nishibori and K. Kinosita, Thin Solid Films **48,** 325 (1978).
10. H.M. Pollock, *ASM Handbook* (ASM International, Metals Park, OH, 1992), Vol. 18, pp. 419–429.
11. W.C. Oliver, MRS Bull. **XI**(5), 15–19 (1986).
12. M.F. Doerner and W.D. Nix, J. Mater. Res. **1,** 601 (1986).
13. E.T. Lilleodden, W. Bonin, J. Nelson, J.T. Wyrobek, and W.W. Gerberick, J. Mater. Res. **10,** 2162 (1995).
14. P. Niedermann, J. Burger, M. Binggeli, R. Christoph, H. Hintermann, and O. Marti, *The Ultimate Limits of Fabrication and Measurements*, edited by M.E. Welland and J.K. Gimzewski (Proc. NATO ARW, Cambridge, England, 1994).
15. N.X. Randall, R. Christoph, S. Droz, and C. Julia-Schmutz, Thin Solid Films **290–291,** 348 (1996).
16. P. Hones, R. Sanjinés, and F. Lévy, Surf. Coat. Technol. **94/95,** 398 (1997).
17. W.C. Oliver and G.M. Pharr, J. Mater. Res. **7,** 1564 (1992).
18. V. Raman and B. Berriche, J. Mater. Res. **7,** 627 (1992).
19. M.J. Mayo and W.D. Nix, in *Strength of Metals and Alloys*, edited by P.O. Kettunen, T.K. Lepistö, and M.E. Lehtonen (Pergamon, Oxford, 1988), p. 1415.
20. N.X. Randall, C. Julia-Schmutz, J-M. Soro, J. Von Stebut, and G. Zacharie, Thin Solid Films **308–309,** 297 (1997).
21. G. Reichardt, F. Eggenstein, U. Flechsig, R. Follath, F. Schäfers, J. Schmidt, and F. Senf, *Groove profiles of soft X-ray diffraction gratings: AFM measurements, efficiency simulations and measurements*, European Workshop on Microtechnology and Scanning Probe Microscopy, 1997.
22. G.F. Samsonov, *The Oxide Handbook*, 2nd ed. (IFI/Plenum, New York, 1982), p. 19.
23. A.S. Kao, M.F. Doerner, and V.J. Novotny, J. Appl. Phys. **66,** 5315 (1989).
24. A.L. Yurkov, J. Mat. Sci. Lett. **12,** 767 (1993).
25. X. Li, D. Diao, and B. Bhushan, Acta Mater. **45,** 4453 (1997).